RESEARCH ARTICLE

Effect of a humic acid colloid on the sorption behaviour of Sr onto soil in a candidate high-level radioactive waste geological disposal site

Rui Zuo[1,2] · Minhua Chen[1,2] · Yuanhui Lin[1,2] · Jie Yang[1,2] · Shuhe Jin[1,2] · Weifeng Yue[1,2] · Jinsheng Wang[1,2] · Yanguo Teng[1,2]

Abstract

We explored the effect of the presence or absence of humic acid (HA) on the sorption behaviour of Sr onto soil. We examined three different experimental cases for Sr sorption: (1) sorption in the presence of only colloidal HA, (2) sorption in the presence of only soil and (3) sorption in the presence of both colloidal HA and soil (HS). A batch technique was used to study the influencing factors, including the amount of colloidal HA, solid content, pH, initial concentration of Sr and contact time. The experiments showed that the influencing factors significantly affected the sorption process. For example, in the case of soil and HS, the sorption percentage increased rapidly with increasing solid content at $m/V < 20$ g/L, changing from 8.35% and 37.54% to 49.09% and 77.03%, respectively. Moreover, scanning electron microscopy and Fourier transform infrared spectroscopy were used to characterize samples. The kinetics and isotherms of Sr were best described by the pseudo-second-order and Langmuir models, which indicated that the process was controlled by chemisorption and uniform monolayer sorption with constant energy on the outer surface. These findings provide valuable information for predicting strontium migration in radioactive waste disposal sites.

Keywords Humic acid colloid · Sr(II) · Soil · Sorption · Geological disposal site

Introduction

With the rapid development of the nuclear industry, nuclear waste disposal and re-pollution issues are becoming a great concern. Geological disposal is the most effective and safe way to dispose of radioactive waste (He et al. 2016). Buried radioactive waste can enter the human environment through geological activities, bioaccumulation and groundwater movement. The Beishan site in Gansu Province in northwestern China is the most likely potential site for a high-level radioactive waste (HLW) repository in China (Wang et al. 2015). The crust in this area possesses a blocky structure,

and the surrounding rocks include metamorphic and sedimentary rocks with Quaternary cover (Zhao et al. 2016).

The ^{90}Sr radionuclide is a typical component of radioactive waste and an important fission product of nuclear weapon testing and reactors (Qi et al. 2015); furthermore, this isotope is recognized as a high-risk radionuclide by the International Atomic Energy Agency (IAEA, 2003). ^{90}Sr has a high mobility in soil/water environment, high heat-generating properties (Ma et al. 2017) and a half-life of 28.8 years. In addition, the chemical properties of Sr are similar to those of Ca, Mg and Ba, and the ability of the human body to distinguish between Sr(II) and Ca(II) is poor. Sr(II) can easily replace Ca(II) and accumulate in the human body, resulting in osteosarcoma, leukaemia and other diseases (Wang et al. 2009). Concerning geochemical behaviour, however, Ba still has a much lower impact on Sr than Ca and Mg because of the high abundance of the latter two cations in natural soils/rocks (Gil-García et al. 2008, 2011). In our study, the Ba content in the soil was lower than the detection limit and was not taken into account in the experimental analysis. Due to the continuous harm caused by Sr to the environment and

✉ Yanguo Teng
   teng1974@163.com

1 College of Water Sciences, Beijing Normal University, Beijing 100875, China

2 Engineering Research Center of Groundwater Pollution Control and Remediation, Ministry of Education, Beijing 100875, China

human health, it is of great significance to use Sr as a representative radionuclide to study the migration of radionuclides into the groundwater environment. Sureda et al. (2010) have performed important research on Sr as a high-level nuclear waste disposal target.

Sorption using solid adsorbents is the preferred method for removing contaminants because it is inexpensive, efficient and convenient (Wang et al. 2009; Kaçan and Kütahyalı 2012). Numerous studies have been performed to remove Sr from aqueous solutions, and several adsorbents have been proposed, such as illite (Missana et al. 2008; Wissocq et al. 2017a; Montoya et al. 2018), attapulgite (Kaygun et al. 2017), natural clayey sandstone (Wissocq et al. 2017b), kaolinite (Başçetin and Atun 2006), montmorillonite (Yu et al. 2015), bentonite colloids (Albarran et al. 2011), Na-rectorite(Zhao et al. 2014) and soil (Schulz et al. 2019); these materials might play an important role in the removal of Sr. However, the sorption of Sr remains highly controversial. Previous studies have confirmed that the contact time, initial concentration of Sr, colloid amount, solid content and pH have an important impact on the results (Rani and Sasidhar 2012; Qi et al. 2015; Shi et al. 2009; He et al. 2016; Nandi et al. 2009; Yu et al. 2015; Zhao et al. 2014; Liu et al. 2015).

The natural colloids in groundwater include inorganic and organic colloids. The most commonly studied colloids include iron oxides and hydroxides (Feng et al. 2013), silica (Saleh et al. 2018; Singer et al. 2014) and humic acid (HA). HA is a major component of naturally occurring organic matter (OM) and is a product of the decomposition of soil OM, which is found extensively in groundwater and soil (Hanudin et al. 2014; Tan et al. 2017). HA has many surface functional groups in its structure (e.g. carboxyl and hydroxyl groups) that act as major coordination sites for clay minerals and metal/radionuclide ions (Zhang et al. 2016). Previous studies have demonstrated that the presence of HA significantly impacts the sorption of nuclides. Yu et al. (2015) and Zhao et al. (2014) showed that HA colloids could strengthen the sorption of Sr onto adsorbents at low pH (less than 7 and 8, respectively); the opposite effect was observed at high pH (greater than 7 and 8.5, respectively). Hence, studying the interaction between HA and soil is significant for simulating the chemical behaviour of soil in the natural environment.

The effect of the presence or absence of HA on Sr sorption onto soil was studied by static batch experiments that explored the impact of various factors (HA colloid amount, solid content, pH, initial concentration of Sr and contact time) on sorption. The sorption mechanism, sorption kinetics and isotherms of Sr on HA and soil were examined. This work provides the necessary research basis for field selection, pollution control and environmental management of HLW geological disposal in China.

Materials and methods

Materials and instruments

Reagent sources HA was purchased from Sinopharm Group Chemical Reagent Co., Ltd., China. Strontium nitrate was obtained from Tianjin Guangfu Fine Chemical Research Institute, China. Hydrochloric acid and sodium hydroxide were purchased from Beijing Beihua Fine Chemicals Co., Ltd., China. All chemicals used in this study were analytically pure.

Soil Representative soil samples were collected from the surface (0–10 cm), consisting of weathered particles, of the Mazongshan Reservoir at the Beishan site. The sampling location is 41° 49′ 17″ N and 97° 00′ 50″ E. The samples were air-dried and cooled to room temperature (25 °C). A portion of each sample was sealed in a bag for physicochemical property testing; the other part was crushed in a mortar and passed through a 1.5-mm sieve.

Stock solution of HA HA was dissolved in 0.5-mol/L sodium hydroxide and then filtered through a 0.45-μm membrane filter. The filtrate was supplemented with 6-mol/L hydrochloric acid, and the pH was adjusted to less than 1.5, at which time the colloid precipitated. The sample was centrifuged at ~400 rpm (38.459g) for 30 min, and the supernatant was removed. The sample was washed with DI water, centrifuged again for 10 min to remove the supernatant, dried, and refrigerated at − 4 °C. A stock colloid of HA (100 mg/L) was formed by adding 0.5-mol/L sodium hydroxide to dissolve the HA solid, and hydrochloric acid was used to adjust the pH to 8. The HA concentration was measured at a wavelength of 350 nm by a spectrophotometer, and the theoretical concentration was approximately 100 mg/L.

Stock solutions of Sr^{2+} Stock solutions of Sr (500 mg/L and 1000 mg/L) were prepared by dissolving Sr(NO$_3$)$_2$ in DI water in a 1000-mL volumetric flask.

Instruments The concentration of the desired stock solution and the concentration of Sr^{2+} in the aqueous solution were determined by inductively coupled plasma atomic emission spectrometry (ICP-AES) (Spectro Arcos Eop, Spectro Analytical Instruments GmbH, USA). Scanning electron microscopy (SEM) (S-4800/EX-350, Hitachi, China) was used to examine the morphologies of HA, soil and HA + soil (HS). The changes in the functional groups before and after mixing soil and HA were characterized using Fourier transform infrared (FTIR) spectroscopy (NEXUS 670, Thermo Fisher Scientific, USA) (KBr powder method). The resolution was set at 4 cm^{-1}, and each

spectrum was the average of 32 scans. A spectrophotometer (GBM, Australia) was used to detect the concentration of HA. The contents of P and Sr in the samples were determined by ICP-AES. Inductively coupled plasma mass spectrometry (ICP-MS) (NexION 300X, PerkinElmer Inc., USA) was used for the determination of Al, Ca, Cu, Fe, K, Mg and Na, and a pH meter (FE20, Mettler Toledo, China) was used to determine the pH value.

Methods

Experimental design To investigate the sorption effect of Sr onto soil in the presence or absence of HA, the experiment was divided into three systems: soil, HA and HS.

Batch sorption experiments Batch sorption tests of Sr onto soil, HA and HS were carried out in sealed 250-mL Erlenmeyer flasks at 25 °C using a thermostatic oscillator (200 rpm) for 24 h. Then, a 10-KDa ultrafiltration membrane was used for filtration, and the concentration of Sr in the filtrate was measured by ICP-AES. Under different experimental conditions, only the influencing parameters were changed, and the other experimental parameters remained constant. The following experiments only describe the HS case; the HA and soil cases were similar. The specific experimental settings are shown in Table 1:

1. Contact time: A total of 20-mL Sr^{2+} stock solution, 100-mL HA and an appropriate amount of DI water were mixed to reach a constant volume (i.e. 1000 mL, Sr concentration = 10 mg/L); then, 20-g soil was added, and the solution was shaken well. The sample was transferred to 1000-mL Erlenmeyer flasks for oscillation times of 10, 20, 60, 120, 300, 600, 1440, 2880 and 4320 min.
2. Initial concentration of Sr: To each of seven 100-mL volumetric flasks was added 10 mL of HA, and then appropriate amounts of Sr^{2+} stock solution and DI water were added to reach a constant volume (i.e. 100 mL) to achieve target initial concentrations of 1, 5, 10, 50, 100, 200 and 500 mg/L. After shaking, the samples were placed in 250-mL Erlenmeyer flasks containing 2-g soil.
3. HA colloid amounts: Volumes of 10, 50 and 100 mL of HA were separately added to 100-mL volumetric flasks. Then, 2 mL of Sr^{2+} stock solution, 2 g of soil and an appropriate amount of DI water were added to reach a constant volume (when the colloid amount was 100 mL, the sorption solution volume was 100 mL by default).
4. Solid contents: Six flasks of 100-mL capacity were added with 2-mL Sr^{2+} stock solution and 10-mL HA. Then, appropriate amounts of soil and DI water were added to reach a constant volume (i.e. 100 mL) to achieve target solid-liquid ratios of 1, 2, 5, 10, 20 and 100 g/L (the Sr^{2+} concentration was 10 mg/L).
5. pH: A total of 20-mL Sr^{2+} stock solution, 100-mL HA and an appropriate amount of DI water were added to reach a constant volume (i.e. 1000 mL, Sr concentration = 10 mg/L). Then, 100-mL aliquots were transferred to beakers, and the pH values of the solutions were carefully adjusted to 3, 4, 5, 6, 7, 8, 9 and 10 using either 0.1-M HCl or 0.1-M NaOH. After shaking, the samples from the beakers were transferred to 250-mL Erlenmeyer flasks containing 2-g soil.

Sorption kinetics To study the sorption kinetics of Sr on soil, HA and HS at different reaction times (10, 20, 60, 120, 300, 600, 1440, 2880 and 4320 min), pseudo-first-order and pseudo-second-order kinetic models were investigated to identify the model that best fit the experimental data.

The pseudo-first-order model assumes that the variation in solute sorption with time is proportional to the saturation concentration and that the amount of solid sorption is proportional

Table 1 Experimental conditions

Variable	Conditions				
	Contact time (min)	Initial concentration of Sr (mg/L)	HA colloid amounts (mL)	Solid contents (g/L)	pH
Contact time (min)	10, 20, 60, 120, 300, 600, 1440, 2880, 4320	10	10	20	7
Initial concentration of Sr (mg/L)	1440	1, 5, 10, 50, 100, 200, 500	10	20	7
HA colloid amounts (mL)	1440	10	10, 50, 100	20	7
Solid contents (g/L)	1440	10	10	1, 5, 10, 20, 100	7
pH	1440	10	10	20	3, 4, 5, 6, 7, 8, 9, 10

to the time. The pseudo-first-order model can be represented as follows (Lagergren 1898):

$$\ln(q_1 - q_t) = \ln q_1 - k_1 t \tag{1}$$

The pseudo-second-order model can be expressed as follows (Weber and Morris 1963):

$$t/q_t = 1/(k_2 q_2^2) + t/q_2 \tag{2}$$

$$h = k_2 q_2^2 \tag{3}$$

where k_1 (min^{-1}) and k_2 (g/(mg min)) are the sorption rate constants, which can reflect the speed of sorption, and a higher sorption rate constant indicates a faster sorption reaction; q_1, q_2 and q_t represent the amounts (mg/g) of Sr adsorbed at the initial time, equilibrium and time t, respectively; and h is the initial sorption rate (mg/(g min)).

The sorption amount and sorption percentage were used to indicate the sorption capacity of the adsorbent and are expressed by the following equations:

$$q_t = (C_0 - C_t) \times V/m \tag{4}$$

$$Y(\%) = (C_0 - C_t)/C_0 \times 100\% \tag{5}$$

where C_0 is the initial liquid-phase Sr concentration (mg/L), C_t is the concentration of Sr (mg/L) at time t, V is the total volume of the solution (L), m is the mass of the adsorbent (g) and Y is the sorption percentage of Sr.

Sorption isotherms Sorption isotherms of Sr on soil, HA and HS for different concentrations of Sr (1, 5, 10, 100, 200 and 500 mg/L) at a contact time of 1440 min were prepared, and the Langmuir and Freundlich models were used to determine the best model to describe the experimental data.

The Langmuir model assumes that the adsorbates undergo chemisorption and monolayer sorption on the surface on a finite number of sites. There is no interaction between the adsorbed molecules, and the model can predict the maximum sorption capacity (Nandi et al. 2009). The equations are as follows:

$$C_e/q_e = 1/(k_L q_m) + C_e/q_m \tag{6}$$

$$R_L = 1/(1 + k_L q_0) \tag{7}$$

where q_0, q_e and q_m are the initial mass concentration, equilibrium sorption capacity and calculated maximum sorption capacity (mg/g) of Sr, respectively; k_L is the sorption equilibrium constant; C_e is the equilibrium concentration of Sr in the solution (mg/L) and R_L is the equilibrium parameter, which can be used to predict the affinity between the adsorbents and adsorbates (Borah et al. 2009) ($R_L = 0$ indicates an irreversible isotherm, $0 < R_L < 1$ indicates a favourable isotherm and $R_L = 1$ indicates an unfavourable isotherm).

The Freundlich isotherm model is an exponential equation suitable for sorption on heterogeneous surfaces that adsorb via intermolecular interactions and is not limited to monolayer formation. The model assumes that the concentration of the adsorbate material on the adsorbent surface increases as the concentration of the adsorbent increases and the energy of the sorption center of the adsorbent exponentially declines. The equation is expressed as follows:

$$q_e = k_F C_e^n \tag{8}$$

Eq (8) can be expressed in linear form:

$$\log(q_e) = \log k_F + n \log(C_e) \tag{9}$$

where q_e is the equilibrium sorption capacity (mg/g) of Sr; C_e is the equilibrium concentration of Sr in the solution (mg/L); k_F (mol^{1-n} L^n/g) represents the reaction capacity when the equilibrium concentration of metal ions is equal to 1 and n represents the dependence degree of sorption on equilibrium concentration (Yang et al. 2009; Nandi et al. 2009). Excel 2016 (Microsoft Corporation, USA) was used for linear fitting of the kinetic and isotherm data.

Results and discussion

Characterization

Physicochemical properties of the samples

The OM content and cationic exchange capacity (CEC) were determined by potassium dichromate oxidation spectrophotometry (HJ615-2011, China) and the barium chloride buffer solution method (SL 237-068-1999, China), respectively. The results are shown in Table 2. As shown in Table 2, Al and Fe have relatively high elemental contents. This result indicates that the possible colloid components in the soil are Al/Fe oxides, hydroxides, organic colloids and organic-inorganic compound colloids bridged by the bivalent or trivalent ions of Al, Fe and organic colloids the three elements. These colloids may act as important components of the sorption of Sr (Li et al. 2017; Wallace et al. 2012). However, the presence of Ca and Mg competes with the sorption of Sr. The soil was slightly acidic, with a low CEC and OM content.

SEM measurements

The surface structures of soil, HA and HS are shown in Fig. 1. The SEM images in Fig. 1 a and d show that HA had a three-dimensional core-shell shape with a smooth surface and a sharp edge (Hui et al. 2009). The particle size was approximately 5 μm. Fig. 1 b and e show that the soil had an uneven size and rough surface. Fig. 1 c and f show that the HA colloid

Table 2   Elemental composition (mg/g), pH, CEC, and OM content of the samples

Al	Ca	Cu	Fe	K	Mg	Na	P	Sr	pH	CEC (cmol/kg)	OM (%)
58.804	37.125	0.028	24.203	24.789	9.135	21.745	0.818	0.194	6.750	3.690	0.590

adhered to the surface of the soil, increasing its surface roughness. This adhesion expanded the layer space and the sorption surface area, which played an important role in explaining the sorption of Sr.

FTIR measurements

To explore the characteristics of the functional groups of the HA colloids and natural soil, FTIR spectra were measured in the range of 4000–400 cm^{-1} (Fig. 2). The HA band at 2922–3055 cm^{-1} is attributed to aliphatic C–H and O–H stretching (Radwan et al. 2015; Hui et al. 2009). The band at 1704 cm^{-1} is attributed to the C=O stretching of carboxyl groups, and the shoulder at 1600 cm^{-1} is attributed to the C=C stretching of aromatic groups; both are characteristic of HA (Hui et al. 2009). The peak at 1418 cm^{-1} is attributed to the O–H bending vibration of carboxylic acids and the stretching vibration of phenols. The C–O stretching vibration and O–H deformation vibration of carboxylic acid functional groups is observed at 1241 cm^{-1}.

The broad peak of soil at 3426 cm^{-1} is attributed to the stretching vibration of O–H, indicating the presence of alcohols and phenols in soil (Luo et al. 2017). The aliphatic C–H stretching vibration was found at 2917 cm^{-1} (Yang et al.

2009). Additionally, the peak at 1629 cm^{-1} represents the stretching of conjugated carbonyls in soil, mainly from ketones and esters. The broad peak at 1440 cm^{-1} is caused by calcite. The strong peak appearing at 1030 cm^{-1} is attributed to tetrahedral Si–O–Si (Yu et al. 2015). The bands at 796 and 873 cm^{-1} are attributed to symmetric vibrations of Si–O–Si (Shi et al. 2009). Moreover, the bands at 520 and 468 cm^{-1} correspond to Al–O–Si and Si–O–Si bending vibrations. Both HA and soil contained O–H and C=O functional groups, which are important for binding Sr (Helal et al. 1998; Deng and Tam 2016; Li et al. 2017).

The FTIR curve of HS was very similar to that of soil, except that the transmittances of the same functional groups were significantly lower at 469, 796, 1030 and 1440 cm^{-1}, and we confirmed that both materials contained the same functional groups.

Sorption kinetics and isotherms

Sorption kinetics

Figure 3 shows the sorption percentages and pseudo-second-order fittings of soil, HA and HS (HA = 10 mL, pH = 7, C_0 = 10 mg/L, m/V = 20:1 g/L). The sorption percentages of soil
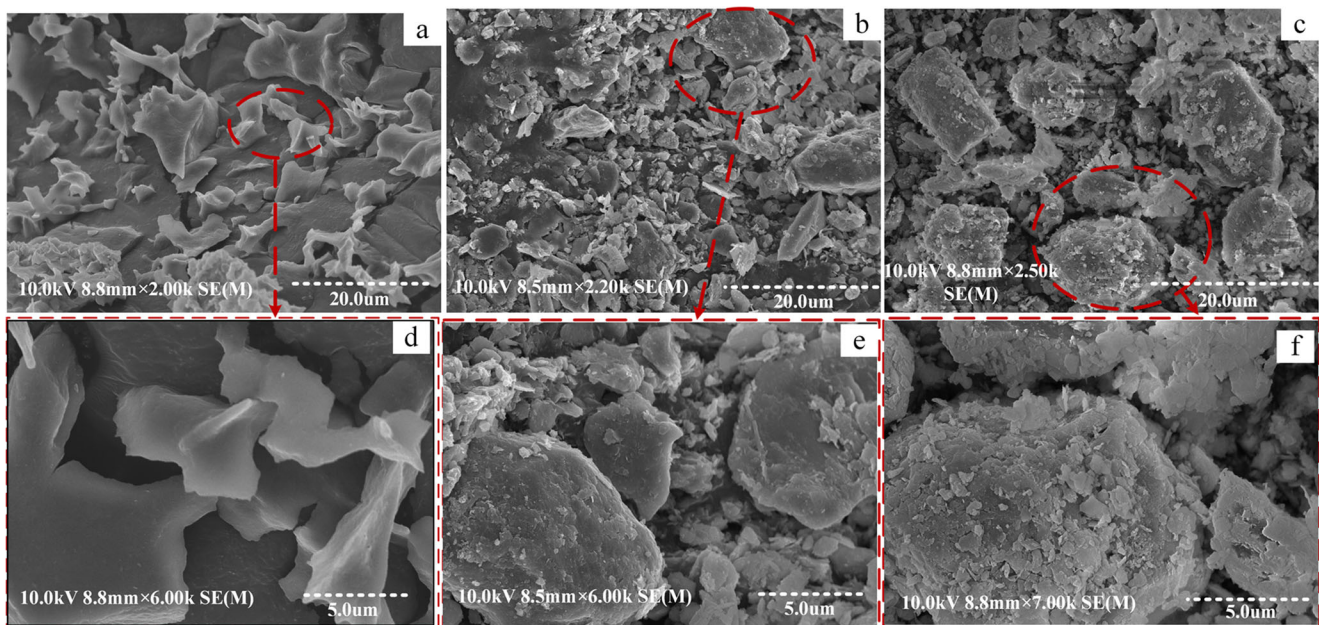

Fig. 1   **a**–**c** SEM micrographs of soil, HA and HS particles at low magnification; the scale bars are 20 μm. **d**–**f** SEM micrographs at higher magnification; the scale bars are 5 μm
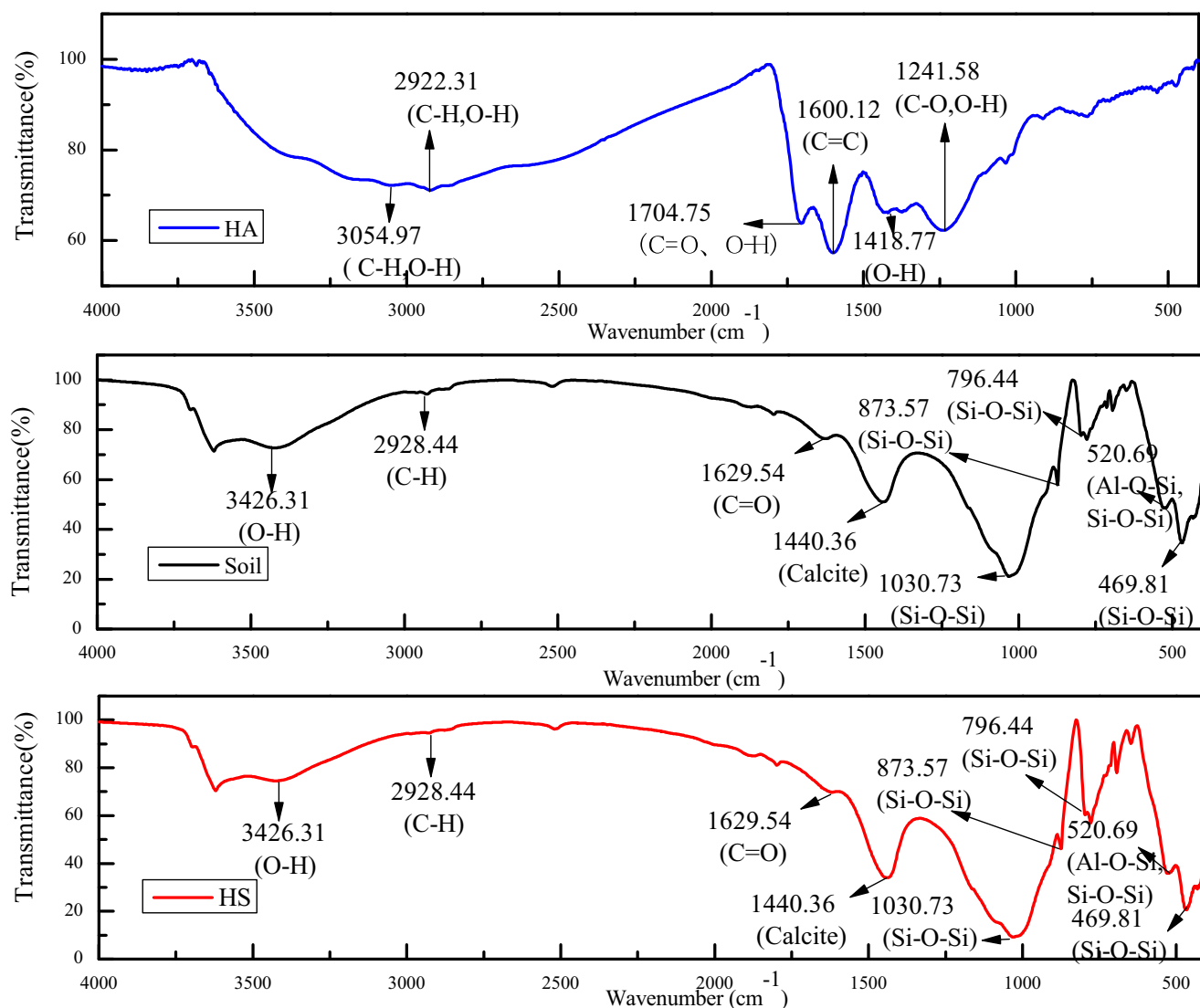
**Fig. 2** FTIR spectra of HA, soil and HS

and HS increased rapidly within 10 h and then became constant at 33.33% and 69.20%, respectively. This rapid reaction within 10 h was mainly dominated by chemisorption of Sr on the particle surface rather than physical sorption (Xiao et al. 2013; Yu et al. 2015). In contrast, the sorption percentage of HA significantly increased in the first 24 h, but 78.26% of the Sr remained in solution. The sorption times required for the three cases were different because Sr, HA and soil combined to form a complex that promoted the completion of the reaction. As the number of exchangeable sites was constant, sorption did not increase when the substrate had been saturated (Schulz et al. 2019; Rani and Sasidhar 2012).

Similar experimental results have been reported for modified graphene materials (Qi et al. 2015), Na-montmorillonite(Yu et al. 2015) and Na-rectorite(Nandi et al. 2009), with equilibration times of 6, 12 and 24 h, respectively. As the sorption properties (composition, structure, etc.) of the

adsorbent materials used in this experiment are different from those of the abovementioned materials, the required equilibrium times are different.

To analyse the sorption rate of Sr on soil, HA and HS, pseudo-first-order and pseudo-second-order kinetic equations were used to fit the data. Table 3 shows the relevant parameters of the two models. By comparing the correlation coefficients R^2, it can be seen that the pseudo-first-order correlation coefficients were between 0.919 and 0.994 and the pseudo-second-order correlation coefficients were between 0.991 and 1.000. This result indicated that the three cases were more consistent with the pseudo-second-order model. The pseudo-second-order model fitting results are shown in Fig. 3. The t/q_t and t curves were straight lines with a slope of $1/q_2$ and an intercept of $1/k_2 \cdot q_2^2$. The calculated q_2 values were very close to the experimental values of q_E, indicating that the process was controlled by chemisorption (Nandi et al. 2009). Similar

Fig. 3 Sorption percentages and pseudo-second-order kinetic fitting results at different contact times. Colloid amount = 10 mL, C_0 = 10 mg/L, pH = 7, m/V = 20:1 g/L
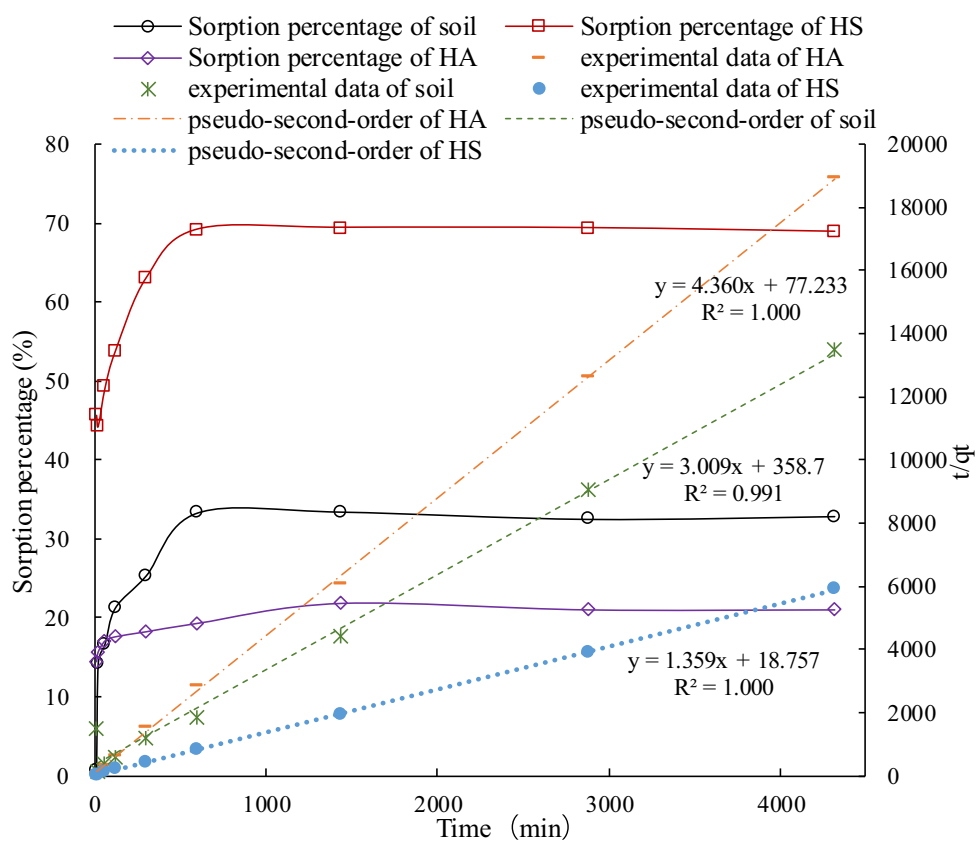
results have been previously reported (Qi et al. 2015; Yu et al. 2015; Zhang et al. 2016; Fan et al. 2008).

Sorption isotherms

Figure 4(a) shows the sorption percentages of Sr onto soil, HA and HS (colloid amount = 10 mL, contact time = 1440 min, pH = 7, m/V = 20:1 g/L); the trends increase first and then stabilize. The amount of removed Sr increased as the concentration of Sr increased to 200 mg/L. However, the Sr sorption percentage decreased as the Sr concentration increased and then remained constant. With increasing concentration from 1 to 500 mg/L, the sorption amount by HA, soil and HS increased from 5.59, 19.70 and 9.86 (10^{-2} mg), respectively, to 78.93, 357.22 and 539.62 (10^{-2} mg), and the sorption

percentage decreased from 86.90%, 46.57% and 87.29% to 1.60%, 6.71% and 10.32%. More Sr was adsorbed by HS, indicating that in the presence of HA, the sorption of high concentrations (> 200 mg/L) of Sr on soil could increase. The sorption saturation concentration of the adsorbent was 200 mg/L.

As the initial concentration of Sr increased, the probability of collisions between Sr and the adsorbent surface increased gradually (Ma et al. 2011), and the amount adsorbed by the adsorbent increased until Sr was bound to all sorption sites. The sorption percentage decreased as the concentration increased, which can be explained by the increasingly fierce sorption competition between Sr and different cations. As the initial concentration increased, the active sites with higher binding energies could fully exert their functions;

Table 3 Relevant parameters of two kinetic models of Sr(II) (10 mg/L) sorption onto soil (2 g), HA (10 mL) and HS (2-g soil + 10-mL HA)

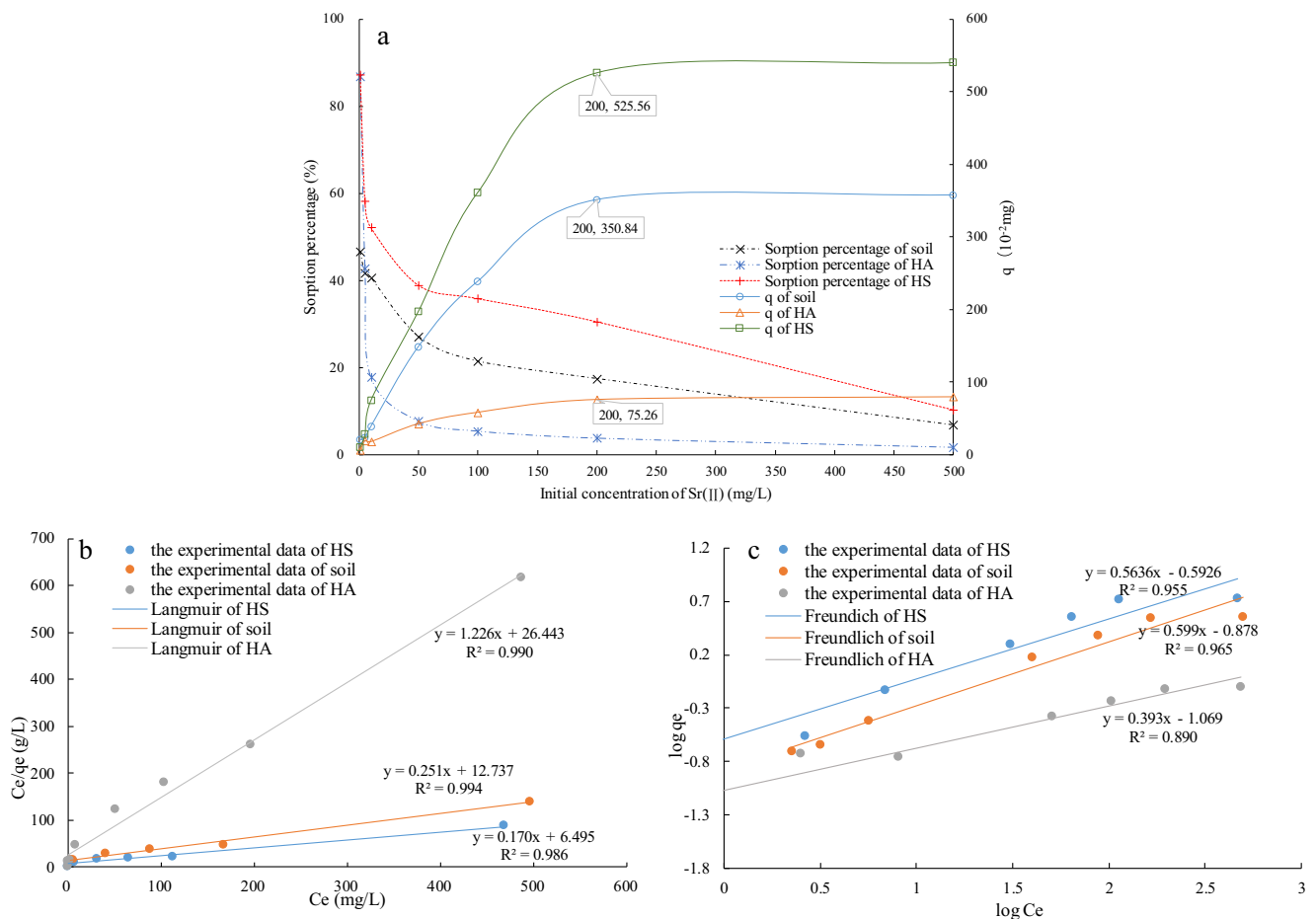| Samples	Pseudo-first-order			Pseudo-second-order				
	R_1^2	q_1 (mg/g)	k_1 (min^{-1})	q_E (mg/g)	R_2^2	q_2 (mg/g)	k_2 (g/mg min)	h (mg/g min)
Soil	0.919	0.176	0.001	0.328	0.991	0.322	0.022	0.003
HA	0.940	0.052	0.001	0.223	1.000	0.231	0.182	0.010
HS	0.994	0.840	0.005	0.739	1.000	0.745	0.071	0.039

Fig. 4 **a** Effect of the initial concentration of Sr on the sorption percentage and sorption capacity. **b** and **c** Langmuir and Freundlich models, respectively, for the sorption of Sr on soil, HA and HS. Colloid amount = 10 mL, contact time = 1440 min, pH = 7, m/V = 20:1 g/L

simultaneously, the binding sites with lower energies gradually participated in sorption. When the initial concentration was more than 200 mg/L, the competitive sorption between Sr atoms was aggravated, and all the available active sites in the solution were fully utilized. Furthermore, the increasing tendency of Sr removal slowed, the sorption percentage remained almost constant and equilibrium was reached (Ali et al. 2016).

To explore the governing sorption isotherm properties, Langmuir and Freundlich models were used to determine the best model to describe the experimental data. The relevant parameters of the two models are listed in Table 4. Figure 4 b and c show that the Langmuir model fits the experimental data better than the Freundlich model. The C_e/q_e and C_e curves are straight lines with a slope of $1/q_m$ and an intercept of $1/(k_L \cdot q_m)$. The R^2 values are 0.994, 0.990 and 0.986, and the maximum sorption capacities are 4.953, 0.816 and 5.879 mg/g, respectively. The maximum sorption q_m derived from the Langmuir model was close to the experimental q_E. It could be speculated that the sorption of Sr on the adsorbents occurred on the

outer surface, providing monolayer sorption with a constant energy and uniform structure. Furthermore, the values of R_L ranged from 0 to 1, which indicated that favourable sorption was achieved for all three cases. The characteristics of the sorption isotherms in this study were consistent with those in previous reports (Fan et al. 2008; Kütahyalı et al. 2012). In contrast, Yu et al. (2015) found that the sorption of Sr on Na-montmorillonite was better described by the Freundlich model. Luo et al. (2017) revealed that the sorption of V on natural soil was better described by the Freundlich model. These results may be related to the type of adsorbent and element, as well as the sorption conditions (Rani and Sasidhar 2012).

Effect of HA on the sorption of Sr

The effect of HA colloid amount (10, 50 and 100 mL) on the sorption of Sr with an initial concentration of 10 mg/L is shown in Fig. 5. In the case of HA, the sorption percentage increased as the amount of HA increased. In the case of soil, only 33.33% sorption was observed. When the colloid amount

Table 4 Relevant parameters of isotherm models of Sr(II) sorption onto soil (2 g), HA (10 mL), and HS (2-g soil +10-mL HA) (sorption solution volume 100 mL)

Samples	Langmuir					Freundlich		
	R_L^2	q_m (mg/g)	q_E (mg/g)	k_L (L/mg)	R_L	R_F^2	k_F (mg/g)	n
Soil	0.994	4.953	3.572	0.020	0.086~0.922	0.965	0.132	0.599
HA	0.990	0.816	0.753	0.046	0.042~0.971	0.890	0.085	0.393
HS	0.986	5.879	5.400	0.026	0.069~0.971	0.955	0.256	0.564

was increased to 50 mL, the sorption percentage of HS was relatively high (76.53%). However, when the colloid amount was increased from 50 to 100 mL, the sorption percentage remained essentially constant (50 mL was considered the optimal amount for sorption). The colloid amount did not affect the equilibrium time, which might be because the sorption equilibrium time of each system was constant under certain conditions (temperature, solid-liquid ratio and initial concentration).

The sorption percentage reached a maximum value of approximately 80% when the amount of HA was 50 mL, as Sr^{2+} was in full contact with the effective sorption sites of HS. However, as the amount of HA increased, more soluble Sr^{2+}-HA complexes formed, which led to a decrease in Sr^{2+} sorption (Yoon et al. 1994). Therefore, 50 mL was considered the optimal addition amount and the amount of HA-soil hybrids reached the maximum. In this case, the effective sorption sites were considered to be fully utilized to achieve complete sorption.

Effect of solid content on the sorption of Sr

Figure 6 shows the sorption of Sr on soil and HS as a function of the solid-liquid ratio (1:1, 5:1, 10:1, 20:1 and 100:1 g/L). The sorption trends of soil and HS were similar with different solid contents. In the case of soil and HS, the sorption percentage increased rapidly with increasing solid content at $m/V <$ 20 g/L, and the sorption percentage increased from 8.35% and 37.54% to 49.09% and 77.03%, respectively. For $m/V > 20$ g/L, the sorption percentage remained essentially constant. The values below the line segments represent the slopes and indicate that the growth rate was the highest when m/V increased from 1:1 to 5:1 and close to zero when m/V increased from 20:1 to 100:1. Therefore, a solid content of 20:1 was optimum for sorption. Fan et al. (2009) and Murali and Mathur (2002) studied the sorption of Ni(II) on Na-attapulgite and the sorption of Sr on bentonite and granite, respectively. Both groups found that sorption increased with solid content and eventually became constant.

Fig. 5 Effect of the amount of HA colloid in soil. Contact time = 1440 min, pH = 7, C_0 = 10 mg/L, m/V = 20:1 g/L
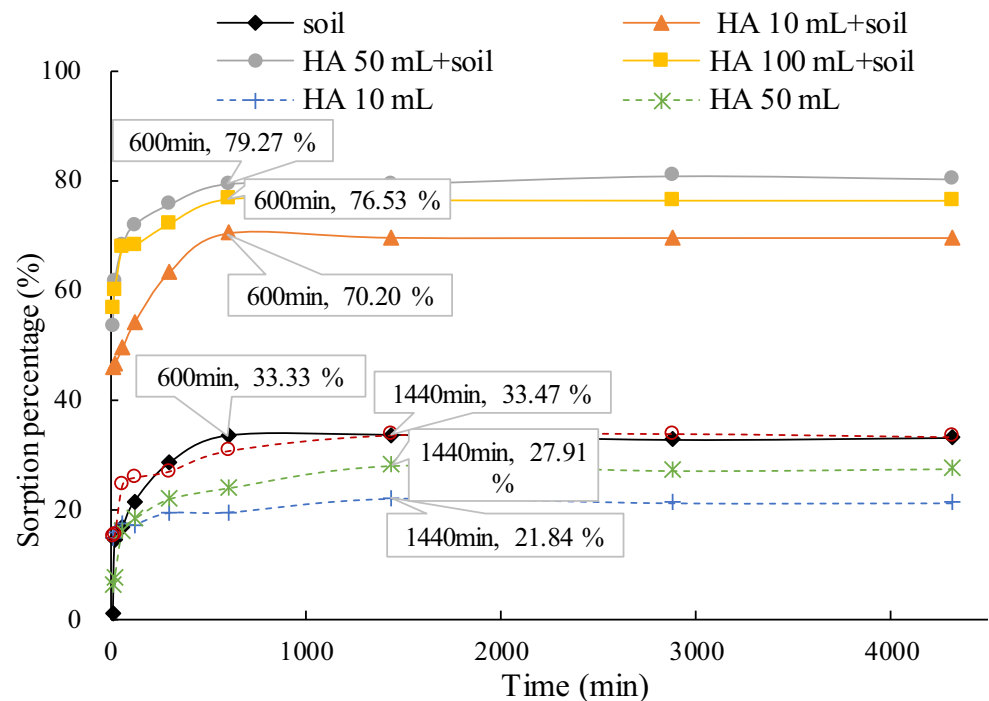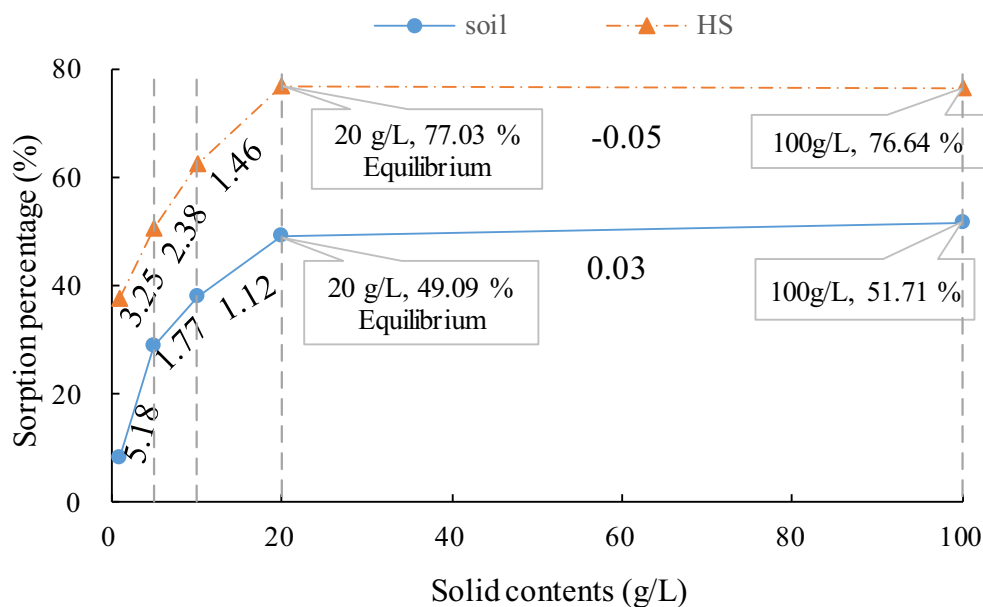
Fig. 6 Effect of solid content in the case of soil and HS. Colloid amount = 10 mL, contact time = 1440 min, pH = 7, C_0 = 10 mg/L


Due to the large contact area and availability of active sorption sites, the sorption of Sr increased with increasing soil content. When the solid content was greater than 20 g/L, the sorption percentage no longer increased, which might be due to the following: (1) a large amount of adsorbent effectively reduced the number of unsaturated sorption sites and decreased the sorption capacity and (2) a higher solid content led to particle aggregation, causing a decrease in the total surface area and increasing the diffusion path length, which contributed to the decrease in the sorption capacity of Sr on soil and HS (Bhattacharyya and Gupta 2008). Therefore, a solid content of 20 g/L was considered to reach saturation. According to Fig. 6, when sorption reached equilibrium, sorption by soil accounted for 2/3 of the sorption percentage of HS, suggesting that soil was the dominant force for the sorption of Sr.

Effect of pH on the sorption of Sr

Figure 7 shows the sorption of Sr onto soil, HA and HS at pH values ranging from 3 to 10. Figure 7 shows that changes in pH have a significant impact on the sorption

Fig. 7 Effect of pH on the sorption of Sr. Colloid amount = 10 mL, contact time = 1440 min, C_0 = 10 mg/L, m/V = 20:1 g/L.
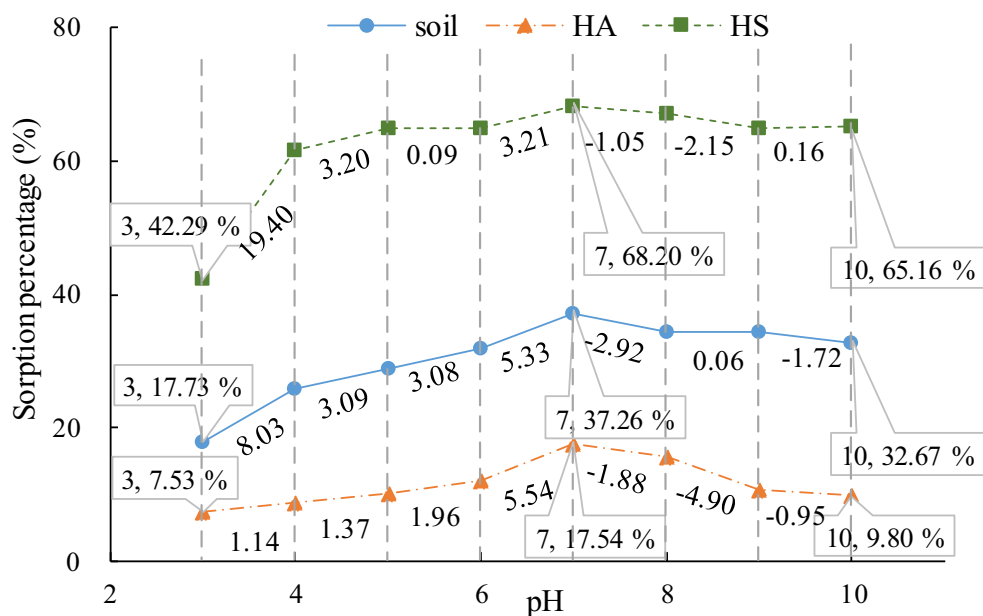
of HA and soil, especially between 3 and 4, but between 4 and 10, the effect is minor, with maximum sorption at pH 7. The values below the line segments indicate the corresponding slopes. Overall, an alkaline environment was more favourable than an acidic environment, and the results were similar to those of other researchers (Tan et al. 2017; Kütahyalı et al. 2012; Ivanova and Spiteller 2014).

The increase in Sr sorption on HS in the low-pH region ($3 < pH < 7$) might be attributed to the decrease in positive surface charge caused by the sorption of negatively charged HA on the surface of soil, which resulted in a more favourable electrostatic environment for Sr^{2+} sorption and enhanced the formation of ternary Sr^{2+}-HA-soil surface complexes. Meanwhile, the surface-attached HA provided more effective groups for the formation of Sr^{2+}-HA complexes and thereby enhanced the sorption of Sr^{2+} on HS. The deprotonation reaction made the soil surface negatively charged at $pH > 7$. Due to electrostatic repulsion, the attachment of negatively charged HA on the soil surface decreased with increasing pH. Therefore, more free HA molecules remained in the solution, and the HA molecules formed soluble Sr^{2+}-HA complexes. This process competitively reduced the sorption of Sr on HS (Xiao et al. 2013). In general, alkaline conditions were more favourable for sorption than acidic conditions.

Conclusion

The results suggest that HA promoted the sorption of Sr in soil. The sorption of Sr on the adsorbent was highly dependent on the amount of HA, solid content and pH. The optimal colloid amount and solid content were 50 mL and 20:1 g/L, respectively. The sorption percentage reached a maximum at $pH = 7$ and decreased as the acidity or alkalinity of the solution increased. Moreover, the FTIR results, solid contents and equilibrium times (24 h for HA and 10 h for soil and HS) revealed that soil played a dominant role in Sr sorption. The initial concentration studies showed that the HS removal efficiency of Sr was approximately 1.5 and 7 times higher than that of soil and HA, respectively. This difference was due to the larger sorption surface and stronger sorption capacity of the complex formed by HA and soil. The sorption behaviour of Sr followed the pseudo-second-order kinetic model and the Langmuir isotherm, demonstrating that the sorption of Sr to the adsorbent was mainly chemisorption and Sr formed a monolayer on the outer surface. This study confirmed that the presence of HA promoted the sorption of Sr onto soil, indicating that the presence of HA has good potential for the treatment of leaked nuclides from HLW.

References

Albarran N, Missana T, García-Gutiérrez M, Alonsoe U, Mingarro M (2011) Strontium migration in a crystalline medium: effects of the presence of bentonite colloids. J Contam Hydrol 122:76–85

Ali R, Hamad H, Hussein M, Malash G (2016) Potential of using green adsorbent of heavy metal removal from aqueous solutions: adsorption kinetics, isotherm, thermodynamic, mechanism and economic analysis. Ecol Eng 91:317–332

Başçetin E, Atun G (2006) Adsorption behavior of strontium on binary mineral mixtures of montmorillonite and kaolinite. Appl Radiat Isotopes 64:957–964

Bhattacharyya KG, Gupta SS (2008) Adsorption of Fe(III), Co(II) and Ni(II) on ZrO–kaolinite and ZrO–montmorillonite surfaces in aqueous medium. Colloids Surf A Physicochem Eng Asp 317(1):71–79

Borah D, Satokawa S, Kato S, Kojima T (2009) Sorption of As (V) from aqueous solution using acid modified carbon black. J Hazard Mater 162:1269–1277

Deng D, Tam N (2016)Adsorption-uptake-metabolism kinetic model on the removal of BDE-47 by a Chlorella isolate. Environ Pollut 212:290–298

Fan Q, Wu W, Song X, Xu J, Hu J, Niu Z (2008) Effect of humic acid, fulvic acid, pH and temperature on the sorption-desorption of Th (IV) on attapulgite. Radiochim Acta 96:159–165

Fan Q, Shao D, Lu Y, Wu W, Wang X (2009) Effect of pH, ionic strength, temperature and humic substances on the sorption of Ni (II) to Na–attapulgite. Chem Eng J 150:188–195

Feng Q, Zhang Z, Chen Y, Liu L, Zhang Z, Chen C (2013) Adsorption and desorption characteristics of arsenic on soils: kinetics, equilibrium, and effect of Fe(OH)$_3$ colloid, H$_2$SiO$_3$ colloid and phosphate. J Environ Sci 18:26–36

Gil-García CJ, Rigol A, Rauret G, Vidal M (2008) Radionuclide sorption–desorption pattern in soils from Spain. Appl Radiat Isotopes 66(2):126–138

Gil-García CJ, Rigol A, Vidal M (2011) The use of hard- and soft-modelling to predict radiostrontium solid–liquid distribution coefficients in soils. Chemosphere 85(8):1400–1405

Hanudin E, Sukmawati ST, Radjagukguk B, Yuwono N (2014) The effect of humic acid and silicic acid on P adsorption by amorphous minerals. Procedia Environ Sci 20:402–409

He Y, Chen YG, Ye WM (2016) Equilibrium, kinetic, and thermodynamic studies of adsorption of Sr (II) from aqueous solution onto GMZ bentonite. Environ Earth Sci 75(9):807

Helal AA, Aly HF, Imam DM, Khalifa SM (1998) Effect of some metal ions on the complexation of strontium with humic acid. J Radioanal Nucl Chem 227(1–2):49–53

HJ615-2011 (2011) Baidu. http://www.doc88.com/p-3197961161257.html

Hui C, Berndtsson R, Ma M, Zhu K (2009) Characterization of insolubilized humic acid and its sorption behaviors. Environ Geol 57:1847–1853

International Atomic Energy Agency (2003) Categorization of radioactive sources. IAEA-TECDOC-1344 IAEA, Vienna

Ivanova B, Spiteller M (2014) Adsorption of uranium composites onto, saltrock oxides—experimental and theoretical study. J Environ Radioact 135:75–83

Kaçan E, Kütahyalı C (2012) Adsorption of strontium from aqueous solution using activated carbon produced from textile sewage sludges. J Anal Appl Pyrol 97:149–157

Kaygun AK, Eral M, Erenturk SA (2017) Removal of cesium and strontium using natural attapulgite: evaluation of adsorption isotherm and thermodynamic data. J Radioanal Nucl Chem 311:1459–1464

Kütahyalı C, Cetinkaya B, Acar M, Is¸ık, N, Cireli I (2012) Investigation of strontium sorption onto Kula volcanics using central composite design. J Hazard Mater 201–202:115–124

Lagergren S (1898) Zur theorie der sogenannten adsorption gelöster stoffe, Kungliga Svenska Vetenskapsakademiens. Handlingar 24(4):1–39

Li M, Liu H, Zhu H, Gao H, Zhang S, Chen T (2017) Kinetics and mechanism of Sr(II) adsorption by Al-Fe₂O₃: evidence from XPS analysis. J Mol Liq 233:364–369

Liu F, Liu Y, Xu Y, Ni L, Meng X, Hu Z, Zhong G, Meng M, Wang Y, Han J (2015) Efficient static and dynamic removal of Sr (II) from aqueous solution using chitosan ion-imprinted polymer functionalized with dithiocarbamate. J Environ Chem Eng 3:1061–1071

Luo X, Yu L, Wang C, Yin X, Mosa A, Lv J, Sune H (2017) Sorption of vanadium (V) onto natural soil colloids under various solution pH and ionic strength conditions. Chemosphere 169:609–617

Ma Z, Li Q, Yue Q, Gao B, Li W, Xu X, Zhong Q (2011) Adsorption removal of ammonium and phosphate from water by fertilizer controlled release agent prepared from wheat straw. Chem Eng J 171: 1209–1217

Ma F, Li Z, Zhao H, Geng Y, Zhou W, Li Q, Zhang L (2017) Potential application of graphene oxide membranes for removal of Cs(I) and Sr(II) from high level-liquid waste. Sep Purif Technol 188:523–529

Missana T, Garcia-Gutierrez M, Alonso U (2008) Sorption of strontium onto illite/smectite mixed clays. Phys Chem Earth 33:156–162

Montoya V, Baeyens B, Glaus MA, Kupcik T, Fernandes MM, Laer LV, Bruggeman C, Maes N, Scha¨fer T (2018) Sorption of Sr, Co and Zn on illite: batch experiments and modelling including Co in-diffusion measurements on compacted samples. Geochim Cosmochim Acta 223:1–20

Murali MS, Mathur JN (2002) Sorption characteristics of Am (III), Sr (II) and Cs (I) on bentonite and granite. J Radioanal Nucl Chem 254: 129–136

Nandi BK, Goswami A, Purkait MK (2009) Adsorption characteristics of brilliant green dye on kaolin. J Hazard Mater 161:387–395

Qi H, Liu H, Gao Y (2015) Removal of Sr (II) from aqueous solutions using polyacrylamide modified graphene oxide composites. J Mol Liq 208:394–401

Radwan E, Ghafar H, Moursy A, Langford C, Bedair A, Achari G (2015) Preparation and characterization of humic acid-carbon hybrid materials as adsorbents for organic micro-pollutants. Environ Sci Pollut Res 22:12035–12049

Rani R, Sasidhar P (2012) Geochemical and thermodynamic aspects of sorption of strontium on kaolinite dominated clay samples at Kalpakkam. Environ Earth Sci 65:1265–1274

Saleh AS, Lee JY, Jo Y, Yun J (2018) Uranium(VI) sorption complexes on silica in the presence of calcium and carbonate. J Environ Radioact 182:63–69

Schulz W, Gupta DK, Beate R, Georg S, Clemens W (2019) Sorption of radiostrontium on various soils. Appl Geochem 101:103–108

Shi T, Jia S, Chen Y, Wen Y, Du C, Guo H, Wang Z (2009) Adsorption of Pb (II), Cr (III), Cu (II), Cd (II) and Ni (II) onto a vanadium mine tailing from aqueous solution. J Hazard Mater 169:838–846

Singer DM, Guo H, Davis JA (2014) U(VI) and Sr(II) batch sorption and diffusion kinetics into mesoporous silica (MCM-41). Chem Geol 390:152–163

SL 237-068-1999(1999) Baidu. https://wenku.baidu.com/view/37bf65d233d4b14e8524683d.html

Sureda R, Martínez-Lladó X, Rovira M, Pablo J, Casas I, Giménez J (2010) Sorption of strontium on uranyl peroxide: implications for a high-level nuclear waste repository. J Hazard Mater 181:881–885

Tan L, Wang X, Tan X, Mei H, Chen C, Hayat T, Alsaedi A, Wen T, Lu S, Wang X (2017) Bonding properties of humic acid with attapulgite and its influence on U (VI) sorption. Chem Geol 464:91–100

Wallace S, Shaw SA, Morris KB, Smoll J, Fuller A, Burker I (2012) Effect of groundwater pH and ionic strength on strontium sorption in aquifer sediments: implications for 90Sr mobility at contaminated nuclear sites. Appl Geochem 27(8):1482–1491

Wang M, Xu L, Peng J, Zhai M, Li J, Wei G (2009) Adsorption and desorption of Sr (II) ions in the gels based on polysaccharide derivates. J Hazard Mater 171:820–826

Wang C, Yang X, Li C, Liu C (2015) The sorption interactions of humic acid onto Beishan granite. Colloid Surface A 484:37–46

Weber WJ, Morris JC (1963) Kinetics of adsorption on carbon from solution. J Sanit Eng Div Am Soc Civ Engrs 89:31–59

Wissocq A, Beaucaire C, Latrille C (2017a) Ca and Sr sorption on Ca-illite: experimental study and modelling. Earth Planet Sci Lett 17: 662–665

Wissocq A, Beaucaire C, Latrille C (2017b) Application of the multi-site ion exchanger model to the sorption of Sr and Cs on natural clayey sandstone. Appl Geochem 93:167–177. https://doi.org/10.1016/j.apgeochem.2017.12.010

Xiao J, Chen Y, Zhao W, Xu J (2013) Sorption behavior of U(VI) onto Chinese bentonite: effect of pH, ionic strength, temperature and humic acid. J Mol Liq 188(12):178–185

Yang S, Li J, Lu Y, Chen Y, Wang X (2009) Sorption of Ni (II) on GMZ bentonite: effects of pH, ionic strength, foreign ions, humic acid and temperature. Appl Radiat Isotopes 67:1600–1608

Yoon TH, Moon H, Park YJ, Park KK (1994) Investigation of metal binding sites on soil fulvic acid using Eu(III) luminescence spectroscopy. Environ Sci Technol 28(12):2139–2146

Yu S, Mei H, Chen X, Tan X, Ahmad B, Alsaedie A, Hayat T, Wang X (2015) Impact of environmental conditions on the sorption behavior of radionuclide 90 Sr (II) on Na-montmorillonite. J Mol Liq 203:39–46

Zhang H, Wang X, Liang H, Tan T, Wu W (2016) Adsorption behavior of Th (IV) onto illite: effect of contact time, pH value, ionic strength, humic acid and temperature. Appl Clay Sci 127–128:35–43

Zhao Y, Shao Z, Chen C, Hu J, Chen H (2014) Effect of environmental conditions on the adsorption behavior of Sr (II) by Na-rectorite. Appl Clay Sci 87:1–6

Zhao XG, Wang J, Chen F, Li P, Ma L, Xie J, Liu Y (2016) Experimental investigations on the thermal conductivity characteristics of Beishan granitic rocks for China's HLW disposal. Tectonophysics 683:124–137